Earthquakes and Structures, *Vol. 13, No. 1 (2017) 17-27*
DOI: https://doi.org/10.12989/eas.2017.13.1.017

Development of nationwide amplification map of response spectrum for Japan based on station correction factors

Yoshihisa Maruyama*[1] and Masaki Sakemoto[2a]

[1]Graduate School of Engineering, Chiba University, 1-33 Yayoi-cho, Inage-ku, Chiba 263-8522, Japan
[2]Nippon Koei Co., Ltd., 1-14-6 Kudankita, Chiyoda-ku, Tokyo 102-8539, Japan

(Received April 5, 2015, Revised May 18, 2017, Accepted July 21, 2017)

Abstract. In this study, the characteristics of site amplification at seismic observation stations in Japan were estimated using the attenuation relationship of each station's response spectrum. Ground motion records observed after 32 earthquakes were employed to construct the attenuation relationship. The station correction factor at each KiK-net station was compared to the transfer functions between the base rock and the surface. For each station, the plot of the station correction factor versus the period was similar in shape to the graphs of the transfer function (amplitude ratio versus period). Therefore, the station correction factors are effective for evaluating site amplifications considering the period of ground shaking. In addition, the station correction factors were evaluated with respect to the average shear wave velocities using a geographic information system (GIS) dataset. Lastly, the site amplifications for specific periods were estimated throughout Japan.

Keywords: attenuation relationship; station correction factor; average shear wave velocity; site amplification

1. Introduction

Ground motion observed at the surface is affected by different influences such as the source characteristics, the propagation path, and the amplification characteristics of the ground surface (Roy and Sahu 2012). The site amplification characteristics affect the intensity of ground motion, and peak ground accelerations (PGAs) and peak ground velocities (PGVs) are mainly used to show the intensity (Worden *et al.* 2010, Bastami and Kowsari 2014). In addition to the intensity of ground motion represented by the PGA and PGV, the periodic contents of ground shaking are also important for evaluating the damage to structures after a large earthquake. To reveal the periodic characteristics of ground shaking, the ratios of PGV to PGA are often investigated using datasets of actual ground motion records (Malhotra 2006). The response spectrum is one of the means to show the periodic contents of ground shaking, and is widely used to represent seismic demand of structures (Fajfar 1999, Makarios 2012). During recent earthquakes in Japan, no severe damage to structures was observed even though the PGA was extremely large. Generally speaking, the PGA strongly depends on short period contents of ground motion, which differ from site to site. Hence, it is essential to consider the periodic characteristics of ground shaking in order to evaluate structural damage (Elenas and Meskouris 2001).

The amplification characteristics of the ground surface has been estimated in several studies for specific geographical areas of Japan as well as the entire area of Japan using GIS datasets based on land classifications from digital national land information (Matsuoka and Midorikawa 1995, Shimizu *et al.* 2006, Yamazaki *et al.* 2000). It is revealed that the amplification factors are correlated with the average shear wave velocity from the surface to a certain depth. The shear wave velocity averaged over the upper 30 m (AVS30) is used for soil classification in the seismic design code in the United States (BSSC 2009). Based on the AVS30 and the classification of geologic units, maps of region-wide site conditions were constructed for California (Wills and Silva 1998); AVS30 is frequently investigated in other seismic prone regions (Kuo *et al.* 2009, Shafiee and Azadi 2007, Gülkan and Kalkan 2002, Lee and Trifunac 2010).

Wakamatsu *et al.* (2004) proposed the Japan Engineering Geomorphologic Classification Map (JEGM) based on a new engineering-based geomorphologic classification scheme. Recently, they extended JEGM, which currently consists of 250 m × 250 m grid cells (Wakamatsu and Matsuoka 2013). The grid cells are categorized by geomorphologic characteristics into 24 classes. A nationwide AVS30 distribution map was created using the nationwide shear wave velocity datasets for Japan, which are available for K-NET (approximately 1,000 sites) and KiK-net (approximately 500 sites) operated by the National Research Institute for Earth Science and Disaster Prevention of Japan survey sites (Okada *et al.* 2004), and JEGM (Wakamatsu and Matsuoka 2013). A nationwide map of amplification factors was constructed taking into account the relationship between AVS30 and the amplification factor of the PGV (Fujimoto and Midorikawa 2006), and it can be downloaded from the Japan Seismic Hazard Information Station (J-SHIS) (Fujiwara *et al.* 2006). Using the map, the spatial distribution of the PGV is

*Corresponding author, Associate Professor
E-mail: ymaruyam@tu.chiba-u.ac.jp
[a]MSc. Eng.

ISSN: 2092-7614 (Print), 2092-7622 (Online)

Table 1 Locations of the epicenters, moment magnitudes, and source depths of the 32 earthquake events used in this study

No.	Date	East longitude	North latitude	Mw	Depth (km)
1	1997.03.26	130.36	31.99	6.0*	8
2	1997.05.13	130.3	31.95	5.9*	8
3	2000.10.06	133.3	35.35	6.6	11
4	2000.10.31	136.34	34.29	5.4*	44
5	2001.03.24	132.7	34.12	6.9	51
6	2001.04.25	132.35	32.79	5.4*	42
7	2003.05.26	141.65	38.82	7.0	71
8	2003.07.26	141.2	38.4	6.2	12
9	2003.09.26	144.08	41.78	8.0	42
10	2004.09.05	136.8	33.03	7.4*	44
11	2004.10.23	138.87	37.29	6.5	13
12	2004.10.27	138.97	37.28	5.8	12
13	2004.11.29	145.28	42.95	6.8	48
14	2004.12.14	141.7	44.08	5.9	9
15	2005.03.20	130.18	33.73	6.6	9
16	2005.07.23	140.13	35.58	5.8*	73
17	2005.08.16	142.28	38.15	7.1	42
18	2006.04.21	139.2	34.93	5.6*	7
19	2006.05.02	139.33	34.92	5.1*	15
20	2006.06.12	131.43	33.13	5.9*	146
21	2006.08.31	140.02	35.63	4.8*	76
22	2007.03.25	136.5	37.3	6.7	11
23	2007.07.16	138.62	37.55	6.7	17
24	2008.05.08	141.95	36.23	6.9	51
25	2008.06.14	140.88	39.03	6.9	8
26	2008.09.11	144.15	41.78	6.8	31
27	2009.08.11	138.5	34.78	6.2	23
28	2010.02.27	128.68	25.92	6.7*	37
29	2011.03.09	143.28	38.33	7.3	8
30	2011.03.11	142.86	38.10	9.0	24
31	2011.04.11	140.67	36.95	6.6	6
32	2011.04.12	140.87	35.48	6.4	26

*The moment magnitude was estimated from the Japan Meteorological Agency's magnitude (*Mj*) using the relationship, $Mw = 0.78Mj + 1.08$ (National Research Institute for Earth Science and Disaster Prevention 2009)

estimated after destructive earthquakes to investigate the relationship between the intensity of ground motion and damage to various structures (Maruyama *et al.* 2010, Shoji *et al.* 2012). The map is also used to obtain the distribution of ground motion intensity at an early stage of an earthquake (Matsuoka and Yamamoto 2012). However, it is difficult to consider the periodic contents of ground shaking only from the distribution of ground motion indices such as the PGA or PGV. In addition, the distribution of ground motion including the periodic effects during a past

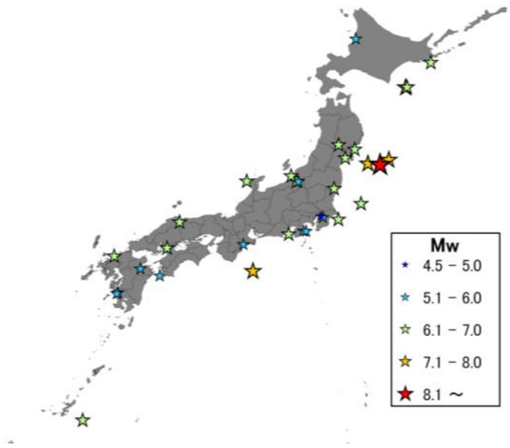

Fig. 1 Locations of epicenters for the 32 earthquake events

earthquake might be helpful to reveal the mechanisms of different structural failures.

Based on these circumstances, we try to develop an amplification map of response spectrum for all of Japan. The AVS30-based site response characteristics are widely used (Anbazhagan *et al.* 2011), and have already been investigated in Japan by Kanno *et al.* (2006). The Tohoku Earthquake off the Pacific coast with a moment magnitude of 9.0 occurred in 2011, and the ground motion records during this event were obtained all over Japan. The earthquake was associated with the largest moment magnitude among those that ever hit Japan. Hence, an empirical approach is newly considered to evaluate the site response characteristics. To achieve this objective, the site amplification characteristics at seismic observation stations are estimated based on the attenuation relationship of its response spectrum (Bozorgnia *et al.* 2010, Lu *et al.* 2010, Gupta 2010) using the K-NET and KiK-net ground motion records. The station correction factors of the attenuation relationships are used to evaluate the site amplification characteristics. Since the plot of the station correction factors for its acceleration response spectrum with respect to the period has some similarity to that for its velocity response spectrum (Shabestari and Yamazaki 1999), we construct the attenuation relationships for the velocity response spectrum with a damping ratio of 5%. To reveal the characteristics of the station correction factors, the station correction factors are compared to the site's transfer functions between the base rock and the ground surface. After obtaining the relationships between the station correction factors and the AVS30, we construct a nationwide amplification map of the velocity response spectrum.

2. Attenuation relationship of response spectrum

We compiled the ground motion records at K-NET and KiK-net stations observed during 32 earthquake events. Table 1 summarizes the earthquake events, and Fig. 1 shows the epicenter locations and the moment magnitudes (Mw). The dataset consists of events that occurred from 1997 to 2011, including the 2011 Tohoku Earthquake off the

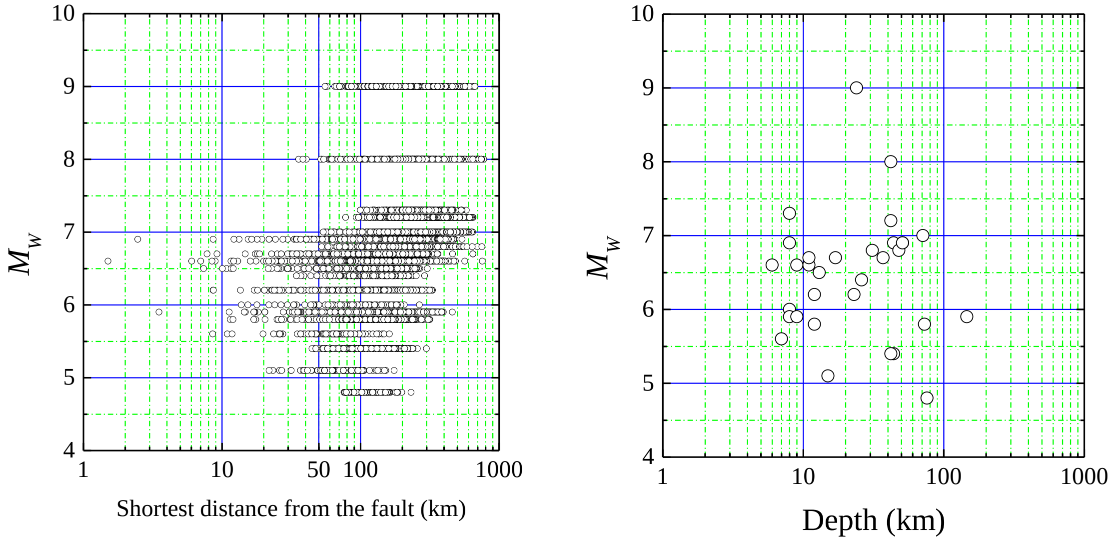

(a) (b)

Fig. 2 Distributions of (a) the distance of the ground motion records from the seismic fault and (b) the hypocentral depths of the 32 earthquakes

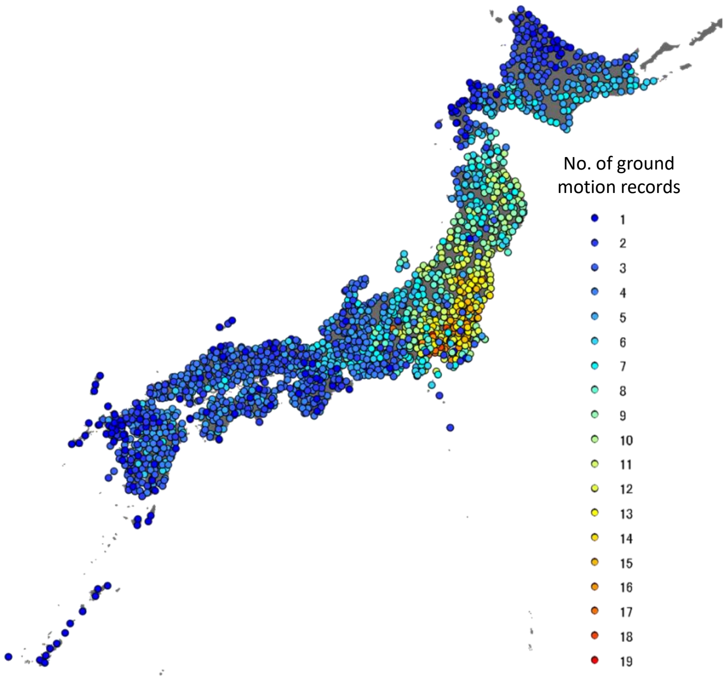

Fig. 3 Locations of K-NET and KiK-net seismic observation stations associated with the number of ground motion records used in this study

Pacific coast with a Mw of 9.0 (No. 30), the 2008 Iwate-Miyagi Inland Earthquake (No. 25), the 2007 Niigata Chuetsu Offshore Earthquake (No. 23), the 2004 Mid Niigata Earthquake (No. 11), and the 2003 Tokachi Offshore Earthquake (No. 9). Fig. 2 shows the distribution of the distances of the ground motion records from (a) the seismic fault and (b) the hypocentral depths. Ground motion records with PGA values less than 5 cm/s^2 for the resultant of the two horizontal components were excluded from the dataset. In the dataset, we have 9,734 ground motion records at 1,699 seismic observation stations, and we use the seismic fault models developed by the Geospatial Information Authority of Japan to calculate the fault distance to each station. Of these records, 130 are associated with fault distances less than 30 km, and 364 have distances less than 50 km. Fig. 3 shows the locations of the K-NET and KiK-net seismic observation stations, labeled with the number of ground motion records used in this study.

Two types of functions of attenuation relationships were assumed in this study

$$\log_{10} y(T) = b_0(T) + b_1(T)Mw + b_2(T)r + b_3(T)\log_{10} r + b_4(T)H + c_i(T) \tag{1}$$

$$\log_{10} y(T) = b_0(T) + b_1(T)Mw + b_2(T)r + b_3(T)\log_{10}(r + k(T)) + b_4(T)H + c_i(T) \tag{2}$$

where $y(T)$ is the amplitude of the velocity response spectra with a damping ratio of 5% in cm/s. The attenuatioin relationships were constructed for the resultant of the two horizontal components ($Sv^H(T)$) and for the vertical component ($Sv^V(T)$). Mw is the moment magnitude, r is the shortest distance from the fault in kilometers, H is the earthquake source depth in kilometers, and the coefficients $b_i(T)$ are determined for each structural period T. The term $c_i(T)$ is the station correction factor for station i, which adjusts for site-specific amplification characteristics for a given period, assuming a mean of zero for all stations. Eq. (1) was assumed following the previous study, and the geometric constant b_3 was assumed to be -1 (Molas and Yamazaki 1995). Eq. (2) was assumed following Si and Midorikawa (2000), and this function takes into account the saturation of amplitude of ground motion in the near-source area by introducing the coefficient $k(T)$. The geometric constant b_3 was also assumed to be -1, and the coefficient $k(T)$ was modeled as

$$k(T) = k_1(T) \cdot 10^{0.5Mw} \tag{3}$$

We performed a series of regression analyses following the schemes mentioned in previous studies (Molas and Yamazaki 1995, Si and Midorikawa 2000) using the 9,734 ground motion records from the 32 earthquakes. Fig. 4 compares the attenuation relationships of velocity response spectra formulated by Eqs. (1) and (2). The attenuation relationships were applied for the Fukushima Inland Earthquake, which occurred on April 11, 2011 with a moment magnitude of 6.6 (No. 31). This event was one of the aftershocks following the 2011 Tohoku Earthquake off the Pacific coast. When the shortest distance from the fault is less than 30 km, differences between Eqs. (1) and (2) are observed owing to the effects of the coefficient $k(T)$.

3. Characteristics of station correction factors

In this study, we focus on the station correction factors to evaluate the site amplification characteristics, $c_i(T)$. First, the station correction factors for the resultant of the two horizontal components obtained from Eqs. (1) and (2) are compared in Fig. 5 to reveal the stability with respect to the regression formula. In the figure, the six seismic observation stations in Tohoku and Kanto districts were selected for comparisons. The results show that the differences between the station correction factors calculated by the two attenuation relationships are so small that the factors estimated by this study can be regarded as stable. Hence, the station correction factors derived from Eq. (2) are employed in this study because they take into account the saturation of amplitude of ground motion in the near-source area.

Fig. 6 compares the regression coefficients of the attenuation relationships for the resultant of the two horizontal components and for the vertical component. The coefficient $k(T)$, as denoted in Eq. (3), is plotted for a moment magnitude of 7.0 in Fig. 6. The differences of the regression coefficients, $b_1(T)$, $b_2(T)$, and $b_4(T)$, for the horizontal and vertical components are small as mentioned in the previous study (Yamazaki and Ansary 1997).

The authors compare the station correction factors with the site's transfer functions. At KiK-net seismic observation stations, accelerometers are installed not only at the ground surface but also in a borehole (Okada *et al.* 2004). Hence, the transfer function between the base rock and the ground surface is calculated as (Katayama *et al.* 1990)

$$H(f) = S_{xy}(f) / S_{xx}(f) \tag{4}$$

where $S_{xx}(f)$ is the power spectrum of the acceleration at the base rock and $S_{xy}(f)$ is the cross spectrum of the acceleration between the base rock and the ground surface. We employed a smoothing technique using a Parzen window with a bandwidth of 0.2 Hz. The ground motion records during the events numbered 29-32 in Table 1 were used to obtain the transfer functions.

The station correction factors of this study were estimated assuming a mean of zero for all stations. Since the transfer functions at KiK-net stations are obtained with reference to the base rock, the station correction factors need to be normalized using the results for very stiff soil conditions. Employing the shear wave velocity profiles at K-NET and KiK-net sations, we selected the ten seismic observation stations listed in Table 2. The AVS30, the shear wave velocity, the thickness of the surface (first) layer, and the shear wave velocity of the second layer are summarized in Table 2. The AVS30 was estimated as

$$AVS30 = 30 / \sum_{i=1}^{n} (H_i / Vs_i) \tag{5}$$

Table 2 Selection of rock sites from K-NET and KiK-net seismic observation stations

Station code	AVS30 (m/s)	Shear wave velocity at surface layer (m/s)	Thickness of the surface layer (m)	Shear wave velocity at the second layer (m/s)
CHBH20	1909.1	1800	18	2100
TCGH17	1432.8	700	6	1450
YMG019	1373.2	250	1	1000
KMWH11	1292.3	400	1	1400
IWTH27	1269.8	240	2	1500
YMGH12	1137.7	380	5	1480
SZOH24	1126.2	360	4	1200
TKYH13	1110.1	130	1	1500
KKWH06	110.24	580	6	1100
MIE014	1009.4	880	5	1040

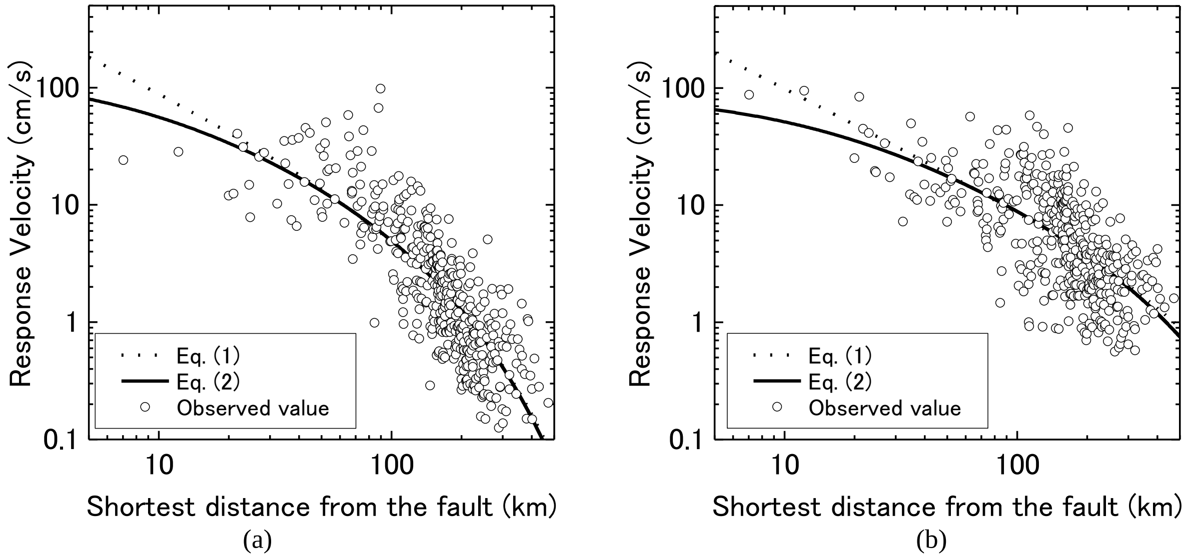

Fig. 4 Attenuation relationships of velocity response spectra with a damping ratio of 5% with a period of (a) 0.2 s and (b) 1.0 s for the Fukushima Inland Earthquake which occurred on April 11, 2011 with a moment magnitude of 6.6

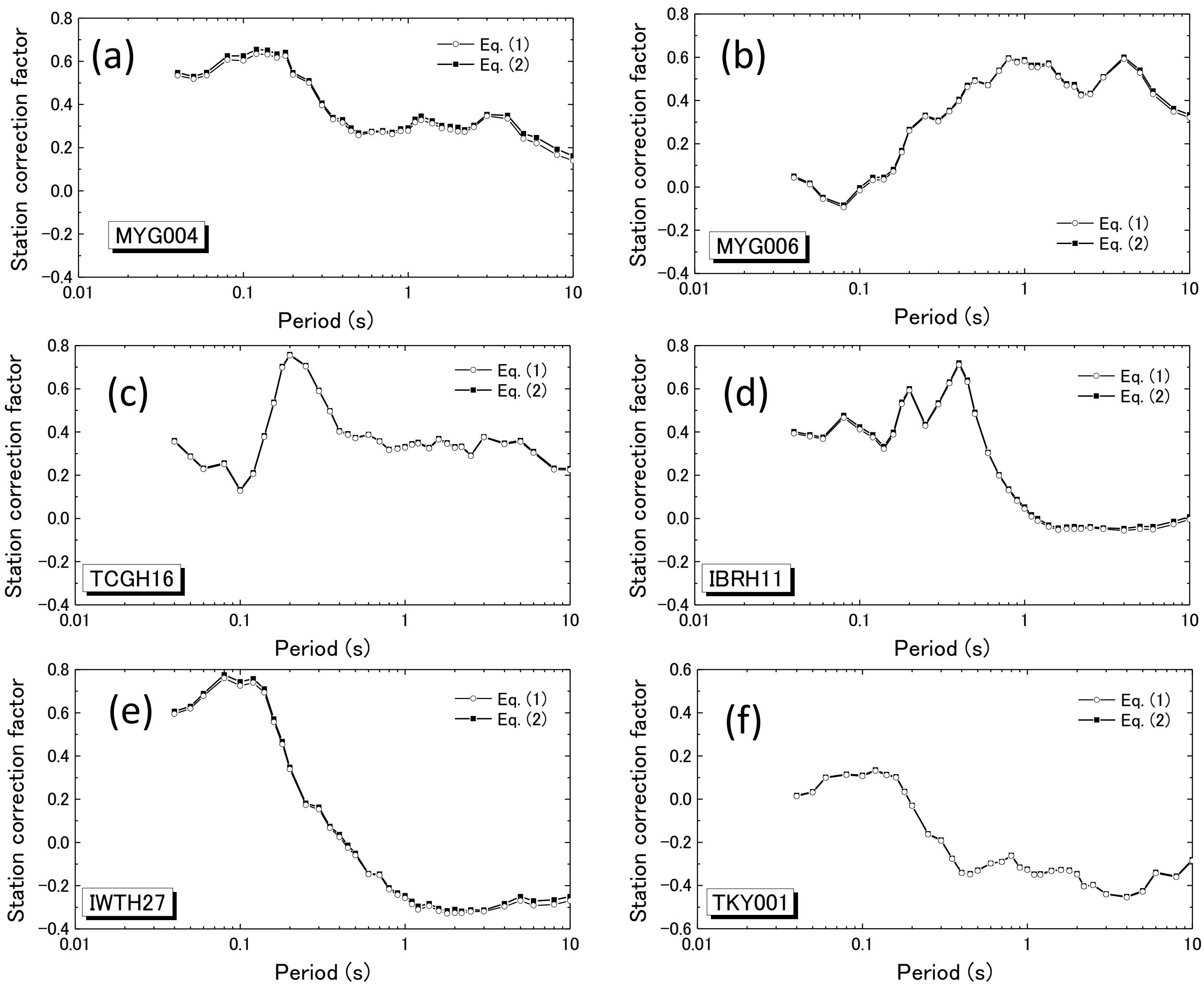

Fig. 5 Comparisons of the station correction factors for the resultant of the two horizontal components estimated from Eqs. (1) and (2) at (a) K-NET Tsukidate, Miyagi Prefecture (MYG004), (b) K-NET Furukawa, Miyagi Prefecture (MYG006), (c) KiK-net Haga, Tochigi Prefecture (TCGH16), (d) KiK-net Iwase, Ibaraki Prefecture (IBRH11), (e) KiK-net Rikuzentakada, Iwate Prefecture (IWTH27), and (f) K-NET Hikawa, Tokyo Metropolis (TKY001)

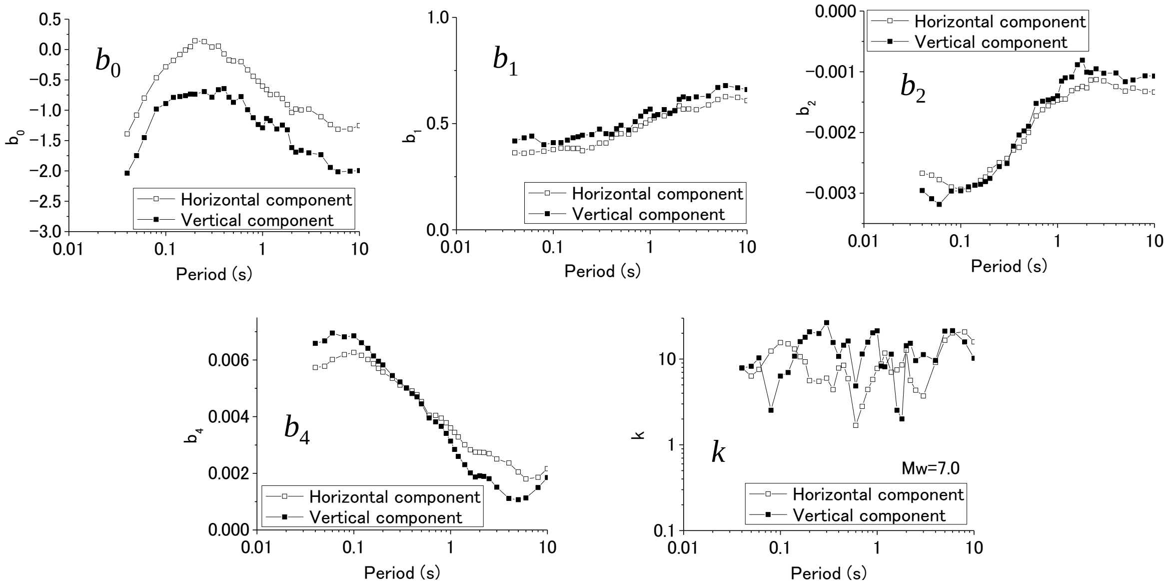

Fig. 6 Regression coefficients of the attenuation relationships of velocity response spectrum for the resultant of two horizontal components and for the vertical component

where H_i and Vs_i are the thickness and shear wave velocity of the i-th layer, respectively.

Fig. 7 shows the station correction factors for the horizontal component at the sites listed in Table 2. We took the mean of these factors, $c_0{}^H(T)$, to normalize the station correction factors. The station correction factors for the horizontal component at KiK-net stations were normalized as Eq. (6), and the normalized factors are compared with the sites' transfer functions in Fig. 8

$$c_i{}'^H(T) = c_i{}^H(T) - c_0{}^H(T) \tag{6}$$

In the figure, we selected the four KiK-net stations located in Tohoku and Kanto districts. As a whole, the plot of station correction factor versus period is similar in shape to that of the transfer functions (amplitude ratio versus period) at that site. The predominant period of the transfer function coincided with that of the station correction factors. The transfer function at IBRH11 (Fig. 8(c)), associated with the earthquake that occurred on April 12, 2011 (No. 32), shows a large amplitude ratio at the period of 0.8 s, but this peak is not observed for the other events. This might be due to the nonlinear effects of soil behavior. These results suggest that station correction factors are effective for evaluating general site amplification versus period during ground shaking. If the effects of nonlinearity on site response are significant, the applicability of the station correction factors should be investigated carefully.

Fig. 9 compares the normalized station correction factors with the ratios of the acceleration response spectra with a damping ratio of 5% at the four KiK-net stations. The vertical axis has a linear scale. The spectral ratio, $SR(T)$ was also estimated using the station correction factors as Eq. (7). The response acceleration spectrum was obtained as the resultant of the two horizontal components, and its ratio was calculated between the base rock and the ground surface. As a whole, the plot of the station correction factor

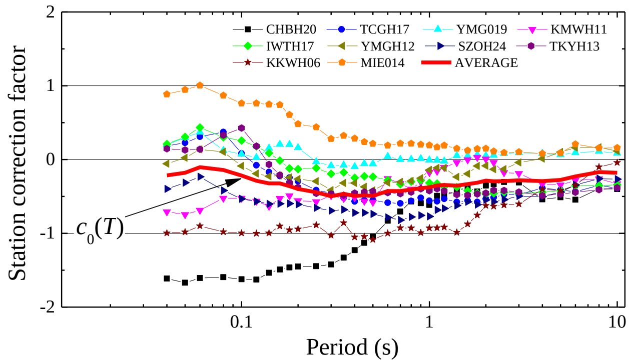

Fig. 7 Station correction factors at the ten rock sites and their mean values

versus period is similar in shape to that of the ratio of the response acceleration spectrum. The station correction factors for the periods shorter than 0.3 s at TKYH12 underestimate the acceleration response spectral ratios (Fig. 9(d))

$$SR(T) = 10^{c_i{}'^H(T)} \tag{7}$$

4. Development of amplification map of response spectrum for all of Japan

The discussion in the previous section indicates that the station correction factors reflect the site response characteristics. The station correction factors obtained in this study have a mean of zero for all the seismic observation stations, and thus it is difficult to assign physical meaning to the reference, such as the shear wave velocity of the reference layer for the station correction factors. Hence, in this study we try to develop the

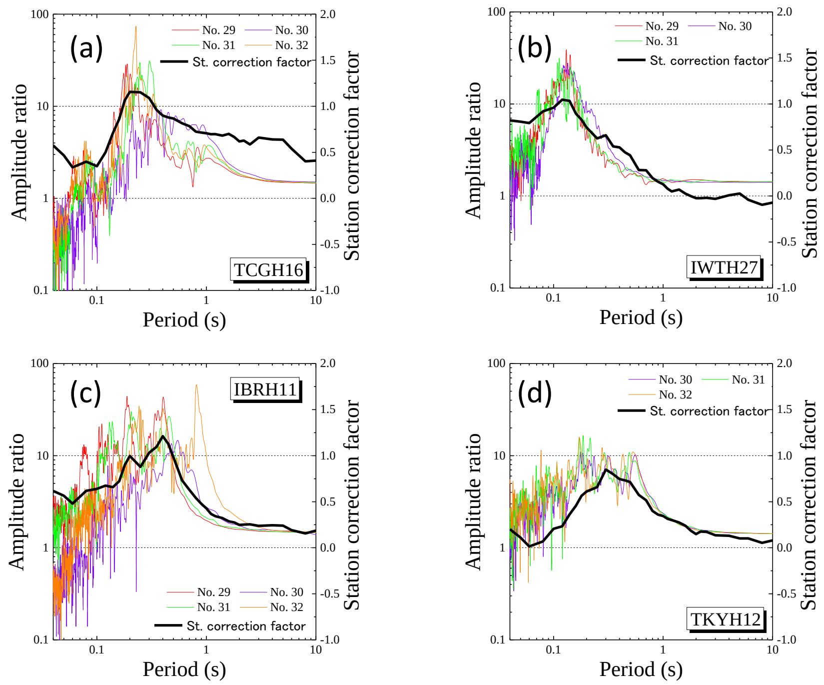

Fig. 8 Comparisons between the station correction factors for the horizontal component and the transfer functions at (a) KiK-net Haga, Tochigi Prefecture (TCGH16), (b) KiK-net Rikuzentakata, Iwate Prefecture (IWTH27), (c) KiK-net Iwase, Ibaraki Prefecture (IBRH11), and (d) KiK-net Hachioji, Tokyo Metropolis (TKYH12)

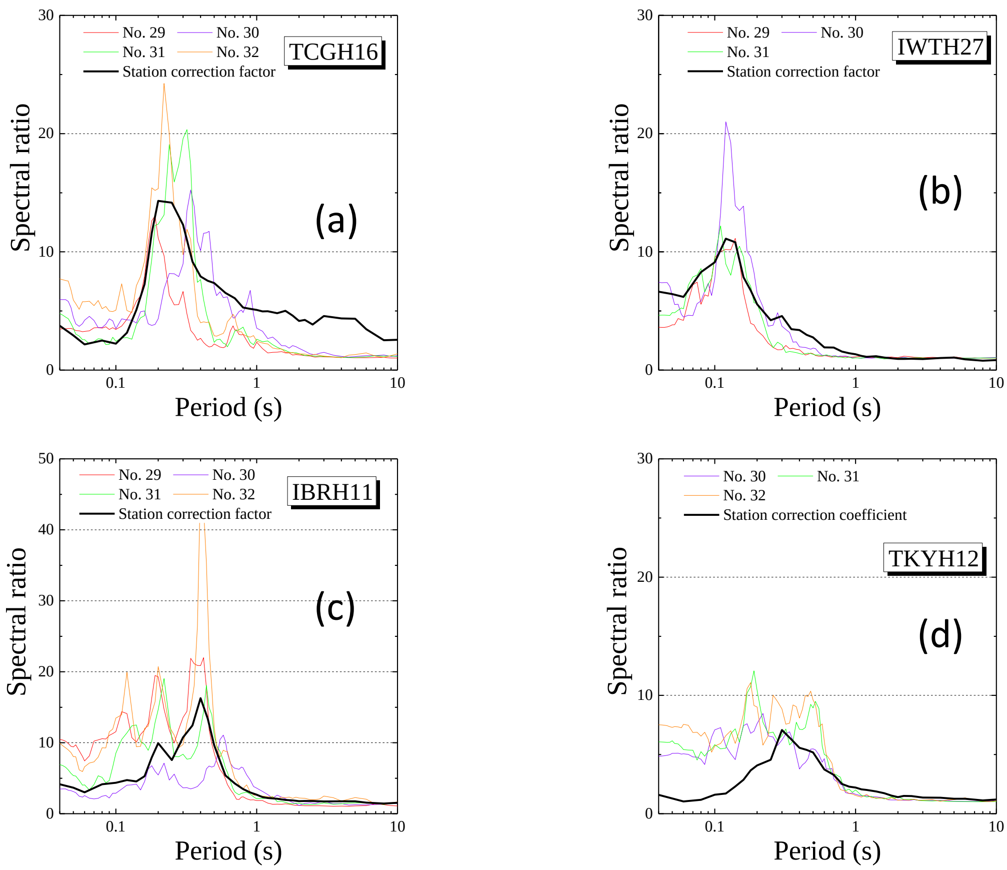

Fig. 9 Comparisons between the station correction factors for the horizontal component and the ratios of the acceleration response spectra at (a) KiK-net Haga, Tochigi Prefecture (TCGH16), (b) KiK-net Rikuzentakata, Iwate Prefecture (IWTH27), (c) KiK-net Iwase, Ibaraki Prefecture (IBRH11), and (d) KiK-net Hachioji, Tokyo Metropolis (TKYH12)

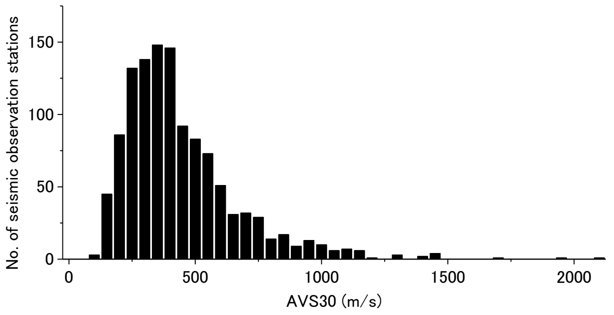

Fig. 10 Histogram of AVS30 for K-NET and KiK-net seismic observation stations used in this study

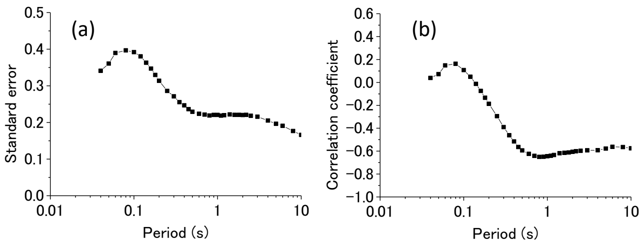

Fig. 11 (a) Standard errors and (b) correlation coefficients between the station correction factors and AVS30 with respect to the period

relationships between the station correction factors for the horizontal component and the AVS30 to define the amplification factors for a given period. Wakamatsu and stations following the same scheme as Wakamatsu and Matsuoka (2013). We then performed a series of regression analyses between the station correction factors, $c_i^H(T)$ and $\log_{10}(AVS30)$ for each given period. Fig. 10 shows the histogram of the AVS30 for K-NET and KiK-net seismic

Matsuoka (2013) illustrated the AVS30 distribution throughout Japan, available at J-SHIS (Fujiwara *et al.* 2006). At K-NET and KiK-net seismic observation stations, shear wave velocity profiles are also available (Okada *et al.* 2004). We calculated AVS30 at the seismic observation observation stations. The maximum and minimum of the AVS30 are 2100 and 84.1 m/s, respectively. The mean of the AVS30 is 417.5 m/s.

Fig. 11 shows the standard errors (*Se*) and correlation coefficients between station correction factors and $\log_{10}(AVS30)$. When the period is longer than 0.5 s, the correlation coefficients are approximately -0.6. The standard errors are approximately 0.2 for the period of 0.5-2.5 s, and they become smaller as the periods become longer. Based on these results, we conclude that the relationships between the station correction factors for periods longer than 0.5 s and AVS30 are effective for estimating the site amplifications. Generally speaking, the short period contents of ground motion strongly depend on the site conditions. The amplification characteristics for periods shorter than 0.5 s are difficult to be explained only by AVS30, and other effects are required for an accurate estimation. Fig. 12 shows the relationships obtained in this study. In the figure, the relationships for periods of 0.5-2.5 s are illustrated, and the 95% confidence intervals denoted as 1.96Se (Ang and Tang 2007) are also shown. The long period contents of ground motion are mainly influenced by the response characteristics of soil deeper than 30 m. The result of this study shows that the AVS30 is highly correlated with the amplification factors for long period contents. The AVS30 may reflect the deeper soil structure conditions, but a further investigation is necessary to draw a solid conclusion. Therefore, this study considers the periodic contents in the range of 0.5-2.5 s.

Fujimoto and Midorikawa (2006) developed the

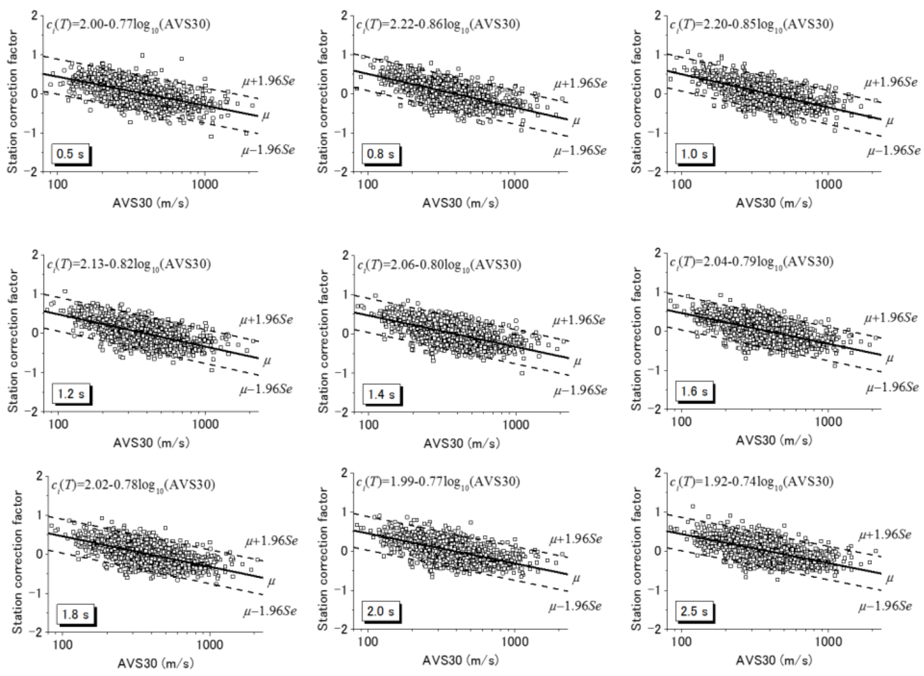

Fig. 12 Relationships between the station correction factors for a given period and AVS30

relationship between the amplification factor of the PGV (AF_{PGV}) and AVS30 using K-NET and KiK-net ground motion records. In their study, they propose Eq. (8) assuming the reference layer with a shear wave velocity of 600 m/s

$$\log_{10} AF_{PGV} = 2.367 - 0.852\log_{10} AVS30 \quad (8)$$

Fig. 13 compares the relationships between the station correction factors for a given period and AVS30. The relationships shown in Fig. 12 were normalized to be zero when the AVS30 is equal to 600 m/s, and they are compared with Eq. (8) in Fig. 13. The relationship between the station correction factors for the period of 1.0 s and AVS30 looks similar to Eq. (8). The standard deviation of Eq. (8) is estimated to be 0.166 (Fujimoto and Midorikawa 2006). In this study, the standard errors associated with longer periods are smaller than 0.2, and the standard error for the period of 10.0 s is approximately 0.166. It is well known that the velocity response spectrum comes close to the PGV as the period becomes longer. This fact resulted in the similarity of the standard deviation of Eq. (8), to the standard errors under longer periods.

Fig. 14 compares the relationships between the AVS30 and amplification factors for the periods of 0.5 and 1.0 s. The Federal Emergency Management Agency (FEMA) and the National Earthquake Hazards Reduction Program (NEHRP) aim to encourage design and building practices that address earthquake hazard and minimize the resulting risk of damage and injury. In the NEHRP Provisions (BSSC 2009), the site factors are introduced for a low-period range (F_a) and a mid-period range (F_v) in terms of the site classifications. The site classifications are defined with respect to the AVS30. We compare the NEHRP site factors with the results of our study with the reference AVS30 of 760 m/s in Fig. 14(a). The effects of amplitude of input motion (S_s and S_l) are considered to show the nonlinear site amplification characteristics in the NEHRP Provisions. The amplifications estimated by our study give larger values when the AVS30 is smaller than 300 m/s for the period of 0.5 s, but are similar to the NEHRP values for the period of 1.0 s.

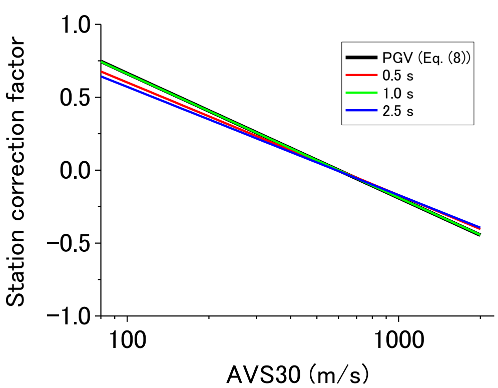

Fig. 13 Relationships between the station correction factors for a given period and AVS30 and the amplification of PGV with respect to AVS30 proposed by Fujimoto and Midorikawa (2006)

Choi and Stewart (2005) also developed formulas for the relationship between the amplification factors for 5% damped response spectral acceleration and the AVS30. In their study, the ground motion records obtained in the U.S. and Turkey were employed. Assuming the reference AVS30 of 760 m/s, we compare the formulas developed by Choi and Stewart (2005) with the results of this study in Fig. 14(b). Kanno *et al.* (2006) considered the site effects as a correction term of the attenuation relationship to improve the accuracy of estimation of ground motion. They developed a formula similar to the one proposed by Choi and Stewart (2005), by including the ground motion records obtained in Japan. Kanno *et al.*'s (2006) formula is also illustrated in Fig. 14(b), and all the relationships are normalized with the reference AVS30 of 760 m/s. No significant differences are observed when the AVS30 is

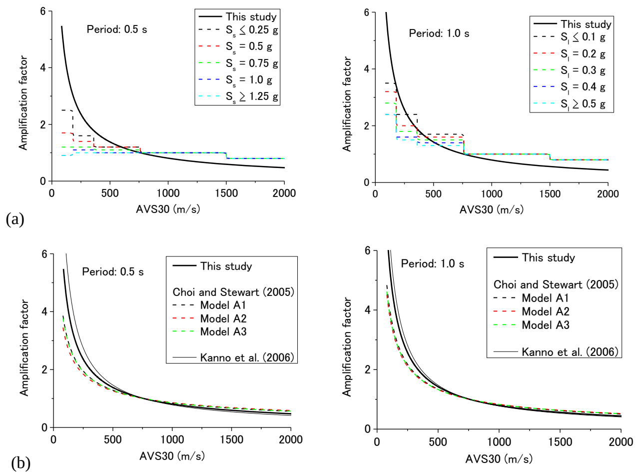

Fig. 14 Estimated amplification factors of response spectrum for given periods by this study compared with those by (a) the NEHRP Provisions, (b) Choi and Stewart (2005), and Kanno *et al.* (2006)

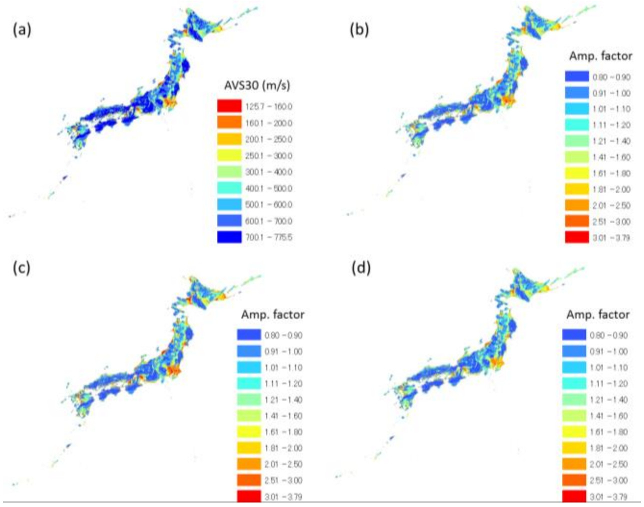

Fig. 15 (a) Distribution of AVS30 throughout Japan, and amplification factors of velocity response spectrum with respect to the reference layer with the shear wave velocity of 600 m/s for periods of (b) 0.5 s, (c) 1.0 s, and (d) 2.5 s

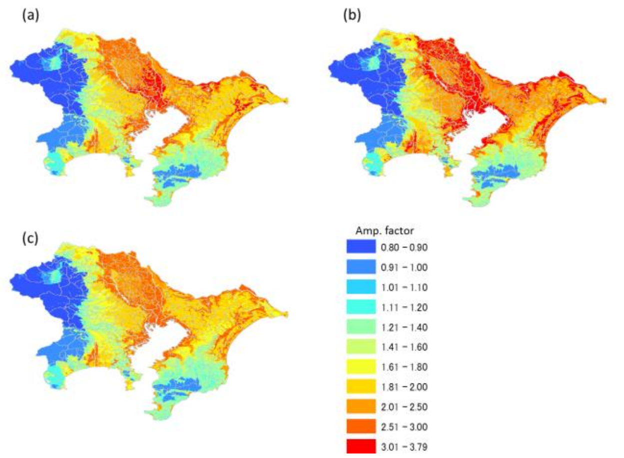

Fig. 16 Distribution of amplification factors of velocity response spectrum with respect to the reference layer with the shear wave velocity of 600 m/s for periods of (a) 0.5 s, (b) 1.0 s, and (c) 2.5 s

larger than 500 m/s. The amplification factors estimated by this study fall between those estimated using the formulas developed by Choi and Stewart (2005) and Kanno *et al.* (2006). Based on these facts, the station correction factors are applicable for estimating the periodic site amplifications.

Employing the distribution of AVS30 throughout Japan developed by Wakamatsu and Matsuoka (2013) and the relationships between the station correction factors and AVS30 shown in Fig. 12, we estimated the amplification factors of the response velocity spectrum with respect to the reference layer with the shear wave velocity of 600 m/s shown in Fig. 15. Fig. 16 shows the distribution of amplification factors with respect to the reference layer in the Tokyo area. The response spectrum with the period of 1.0 s is much amplified in the middle of the region and in the area along Tokyo Bay.

5. Conclusions

In this study, we investigated how to estimate the site response characteristics using the station correction factors of attenuation relationships for the response spectrum. To this end, 9,734 ground motion records at 1,699 seismic observation stations during 32 earthquake events were employed, and the attenuation relationships for the velocity response spectrum with a damping ratio of 5% were constructed. We obtained station correction factors for the 1,699 seismic observation stations, and evaluated them with respect to the shear wave velocity averaged over the upper 30 m (AVS30).

We then compared the station correction factors with their respective transfer functions, which represent the amplification characteristics between the base rock and the surface at KiK-net seismic observation stations. Our results show that, for each station, the plot of station correction factor versus period is similar in shape to the plotted transfer functions for that station. Therefore, the station correction factors are effective for evaluating site amplification versus period during ground shaking. We evaluated the station correction factors with respect to the AVS30, and performed regression analyses to construct the linear relationships between the $\log_{10}(AVS30)$ and the station correction factors for specific periods. The obtained relationships were compared with those of previous studies. No significant differences were observed, and the amplification factors estimated by this study are spread between the relationships developed by the previous studies.

Based on these findings, the station correction factors are applicable in estimating periodic site amplifications. Lastly, we constructed a map showing the nationwide distributions of amplification factors of response spectrum for specific periods. The periodic contents of ground shaking can be estimated using these amplification maps.

In future studies, the nonlinear effects of surface soil need to be properly treated. In this study we constructed the attenuation relationships by including the ground motion records with large amplitudes associated with large magnitude events to consider the effects of nonlinearity. However, disagreements were observed in some cases when the station correction factors are compared with the transfer functions under actual intense ground motion records. To solve this problem, we need to know the extent of nonlinear effects due to soil conditions. Then, the attenuation relationships can be separately constructed to obtain the station correction factors based on the ground motion records with and without the effects of nonlinearity. Lastly, earthquake induced damage to various structures can be evaluated with emphasis on periodic contents of ground shaking employing the amplification maps.

References

Ang, A.H.S. and Tang, W.H. (2007), *Probability concepts in engineering*, Wiley.

Anbazhagan, P., Aditya, P. and Rashmi, H.N. (2011), “Amplification based on shear wave velocity for seismic zonation: comparison of empirical relations and site response results for shallow engineering bedrock sites”, *Geomech. Eng.*, **3**(3), 189-206.

Bastami, M. and Kowsari, M. (2014), “Seismicity and seismic hazard assessment for greater Tehran region using Gumbel first asymptotic distribution”, *Struct. Eng. Mech.*, **49**(3), 355-372.

Bozorgnia, Y., Hachem, M.M. and Campbell, K.W. (2010), “Ground Motion Prediction Equation (“Attenuation Relationship”) for Inelastic Response Spectra”, *Earthq. Spectra*, **26**(1), 1-23.

Building Seismic Safety Council (BSSC). (2009), “NEHRP recommended seismic provisions for new buildings and other structures”, FEMA, Washington DC.

Choi, Y. and Stewart, J.P. (2005), “Nonlinear site amplification as function of 30 m shear wave velocity”, *Earthq. Spectra*, **21**(1), 1-30.

Elenas, A. and Meskouris, K. (2001), “Correlation study between seismic acceleration parameters and damage indices of structures”, *Eng. Struct.*, **23**(6), 698-704.

Fajfar, P. (1999), “Capacity spectrum method based on inelastic demand spectra”, *Earthq. Eng. Struct. D.*, **28**(9), 979-993.

Fujimoto, K. and Midorikawa, S. (2006) “Empirical estimates of site amplification factor from strong-motion records at nearby station pairs", *Proceedings of the 1st European Conference on Earthquake Engineering and Seismology*, Paper No. 251.

Fujiwara, H., Kawai, S., Aoi, S., Ishii, T., Okumura, T., Hayakawa, Y., Morikawa, N., Senna, S., Kobayashi, K. and Hao, K. (2006), "Japan seismic hazard information station, J-SHIS", *Proceedings of the 4th International Conference on Earthquake Engineering*, Paper No. 274.

Gülkan, P. and Kalkan, E. (2002), "Attenuation modeling of recent earthquakes in Turkey", *J. Seismol.*, **6**(3), 397-409.

Gupta, I.D. (2010), "Response spectral attenuation relations for in-slab earthquakes in Indo-Burmese subduction zone", *Soil Dyn. Earthq. Eng.*, **30**(5), 368-377.

Kanno, T., Narita, A., Morikawa, N., Fujiwara, H. and Fukushima, Y. (2006), "A new attenuation relation for strong ground motion in Japan based on recorded data", *Bull. Seismol. Soc. Am.*, **96**(3), 879-897.

Katayama, T., Yamazaki, F., Nagata, S., Lu, L. and Turker, T. (1990), "A strong motion database for the chiba seismometer array and its engineering analysis", *Earthq. Eng. Struct. D.*, **19**(8), 1089-1106.

Kuo, C.H., Cheng, D.S., Hsieh, H.H., Chang, T.M., Chiang, H.J., Lin, C.M. and Wen, K.L. (2009), "Comparison of three different methods in investigating shallow shear-wave velocity structures in Ilan, Taiwan", *Soil Dyn. Earthq. Eng.*, **29**(1), 133-143.

Lee, V.W. and Trifunac, M.D. (2010), "Should average shear-wave velocity in the top 30m of soil be used to describe seismic amplification?", *Soil Dyn. Earthq. Eng.*, **30**(11), 1250-1258.

Lu, D., Cui, J., Li, X. and Lian, W. (2010), "Ground motion attenuation of Ms8.0 Wenchuan earthquake", *Earthq. Sci.*, **23**(1), 95-100.

Makarios, K.T. (2012), "Evaluating the effective spectral seismic amplification factor on a probabilistic basis", *Earthq. Struct.*, **8**(2), 121-129.

Malhotra, P.K. (2006), "Smooth spectra of horizontal and vertical ground motions", *Bull. Seismol. Soc. Am.*, **96**(2), 506-518.

Maruyama, Y., Yamazaki, F., Mizuno, K., Tsuchiya, Y. and Yogai, H. (2010), "Fragility curves for expressway embankments based on damage datasets after recent earthquakes in Japan", *Soil Dyn. Earthq. Eng.*, **30**(11), 1158-1167.

Matsuoka, M. and Midorikawa, S. (1995) "GIS-based integrated seismic hazard mapping for a large metropolitan area", *Proceedings of the 5th International Conference on Seismic Zonation*, **2**, 1334-1341.

Matsuoka, M. and Yamamoto, N. (2012), "Web-based quick estimation system of strong ground motion maps using engineering geomorphologic classification map and observed seismic records", *Proceedings of the 15th World Conference on Earthquake Engineering*, Paper No. 4016.

Molas, G.L. and Yamazaki, F. (1995), "Attenuation of earthquake ground motion indices in Japan including deep focus events", *Bull. Seismol. Soc. Am.*, **85**(5), 1343-1358.

National Research Institute for Earth Science and Disaster Prevention, Japan. (2009), *Technical reports on national seismic hazard maps for Japan*.

Okada, Y., Kasahara, K., Hori, S., Obara, K., Sekiguchi, S., Fujiwara, H. and Yamamoto, A. (2004), "Recent progress of seismic observation networks in Japan - Hi-net, F-net, K-NET and KiK-net", *Earth, Planets, and Space*, **56**(8), 15-28.

Roy, N. and Sahu, R.B. (2012), "Site specific ground motion simulation and seismic response analysis for microzonation of Kolkata", *Geomech. Eng.*, **4**(1), 1-18.

Shabestari, K.T. and Yamazaki, F. (1999), "Attenuation relation of strong ground motion indices using K-NET records", *Proceedings of The 25th JSCE Earthquake Engineering Symposium*, **1**, 137-140.

Shafiee, A. and Azadi, A. (2007), "Shear-wave velocity characteristics of geological units throughout Tehran City, Iran", *J. Asian Earth Sci.*, **29**(1), 105-115.

Shimizu, Y., Yamazaki, F., Yasuda, S., Towhata, I., Suzuki, T., Isoyama, R., Ishida, E., Suetomi, I., Koganemaru, K. and Nakayama, W. (2006), "Development of real-time control system for urban gas supply network", *J. Geotech. Geoenviron. Eng.*, ASCE, **132**(2), 237-249.

Shoji, G., Takahashi, D., Tsukiji, T. and Naba, S. (2012), "Damage assessment on electric power failures during the 2011 off the Pacific coast of Tohoku earthquake", *Proceedings of the International Symposium on Engineering Lessons Learned from the 2011 Great East Japan Earthquake*, 1552-1559.

Si, H. and Midorikawa, S. (2000), "New attenuation relations for peak ground acceleration and velocity considering effects of fault type and site condition", *Proceedings of the 12th World Conference on Earthquake Engineering*, CD-ROM, 8p.

Wakamatsu, K., Matsuoka, M., Hasegawa, K., Kubo, S. and Sugiura, M. (2004) "GIS-based engineering geomorphologic map for nationwide hazard assessment", *Proceedings 11th International Conference on Soil Dynamics & Earthquake Engineering and 3rd International Conference on Earthquake Geotechnical Engineering*, **1**, 879-886.

Wakamatsu, K. and Matsuoka, M. (2013), "Nationwide 7.5-arc-second Japan engineering geomorphologic classification map and Vs30 zoning", *J. Disaster Res.*, **8**(5), 904-911.

Wills, C.J. and Silva, W. (1998), "Shear-wave velocity characteristics of geologic units in California", *Earthq. Spectra*, **14**(3), 533-556.

Worden, C.B., Wald, D.J., Allen, T.I., Lin, K., Garcia, D. and Cua, G. (2010), "A revised ground-motion and intensity interpolation scheme for ShakeMap", *Bull. Seismol. Soc. Am.*, **100**(6), 3083-3096.

Yamazaki, F. and Ansary, M.A. (1997), "Horizontal-to-vertical spectrum ratio of earthquake ground motion for site characterization", *Earthq. Eng. Struct. D.*, **26**(7), 671-689.

Yamazaki, F., Wakamatsu, K., Onishi, J. and Shabestari, K.T. (2000), "Relationship between geomorphological land classification and soil amplification ratio based on JMA strong motion records", *Soil Dyn. Earthq. Eng.*, **19**(1), 41-53.

CC